DIRICHLET BOUNDARY CONTROL OF A STEADY MULTISCALE FLUID-STRUCTURE INTERACTION SYSTEM

Giacomo Barbi[1], Andrea Chierici[2], Valentina Giovacchini[1], Luigi Manes[1], Sandro Manservisi[1] and Lucia Sirotti[1]

[1]University of Bologna - DIN, Via dei Colli 16, 40136 Bologna (BO), Italy
[2] Department of Mathematics and Statistics, Texas Tech University, Lubbock, TX 79409, USA
e-mail: valentin.giovacchin2@unibo.it

Key words: Optimal Boundary Control, Adjoint Variables, Multiscale FSI

Abstract. This work aims to extend the techniques used for the optimal control of the Navier-Stokes systems to control a steady multi-scale FSI system. In particular, we consider a multi-scale fluid-structure interaction problem where the structure obeys a membrane model derived from the Koiter shell equations. With this approach, the thickness of the solid wall can be neglected, with a meaningful reduction of the computational cost of the numerical problem. The fluid-structure simulation is then reduced to the fluid equations on a moving mesh together with a Robin boundary condition imposed on the moving solid surface. The inverse problem is formulated to control the velocity on a boundary to obtain a desired displacement of the solid membrane. For this purpose, we use an optimization method that relies on the Lagrange multiplier formalism to obtain the first-order necessary conditions for optimality. The arising optimality system is discretized in a finite element framework and solved with an iterative steepest descent algorithm, used to reduce the computational cost of the numerical simulations.

1 INTRODUCTION

In this work, we study the optimal control of a fluid-structure system, where the solid is modeled with a multiscale model. The fluid-structure interaction (FSI) simulations have gained popularity and interest in the research community thanks to the large variety of possible applications. In such numerical problems, the fluid flow changes the tensional state of a solid structure and, at the same time, the solid deformation affects the fluid flow. Several models have been implemented to represent the behavior of the interaction between a fluid and a solid, and a large variety of articles and books is available on this topic [1, 2].

We consider a fluid-structure multiscale model, based on the reduction of the dimensionality of the solid, through the so-called Koiter shell equations firstly presented in [3]. To couple the fluid and the structure domains, the Koiter shell equations are embedded into the fluid equations as a Robin boundary condition [4]. By using this model, which has many applications in cases where a fluid interacts with a thin membrane, the optimal control system is easier to obtain.

To control the presented FSI system, an adjoint-based method is used. Such a method has been proven to be a good approach for the optimal control of complex computational fluid dynamics problems [5]. Moreover, these methods have a solid mathematical background and

the existence of local optimal solutions can be proven for many interesting cases [6]. Many works deal with adjoint FSI optimization, such as [7, 8] and references therein. In particular, in [9] an optimal pressure boundary control problem for a steady multiscale fluid-structure interaction system has been presented. In this paper we solve a stationary displacement matching problem: the control variable is the fluid velocity on a boundary, and we use the Lagrangian multipliers method to obtain the optimality system, and to reproduce a desired displacement in a target region of the domain.

Moreover, we focus on the regularity of the optimal solution on the controlled boundary. In fact, the presence of fractional norms can occur in the treatment of boundary optimal control problems. These norms lead to the presence of fractional derivatives in the first-order necessary conditions that characterize optimal solutions. To deal with the issue of balanced regularity [10], we implement a numerical algorithm for the simulation of fractional operators on the controlled boundary of the domain, obtaining optimal solutions in the correct functional space.

The rest of this paper is organized as follows. In Section 2 we introduce the mathematical and physical model describing the considered multiscale FSI problem. In Section 3 the optimal control problem is introduced and we derive the optimality system arising from the minimization of the augmented Lagrangian. Moreover, we introduce the regularization of the presented optimal control problem in the fractional Sobolev space, in order to deal with the balanced regularity issue. In Section 4, the implemented numerical algorithm is presented, and the finite element formulation for the fractional operator is reported. Then, some numerical results are shown.

2 Physical model

In this section, the mathematical model for FSI problem is introduced. While the fluid is modeled with the standard Navier-Stokes equations, a shell model is used for the solid modeling. In particular, the structural model is based on the Koiter shell approach that considers the model of an elastic thin membrane.

In the following, we denote with $L^2(\Omega)$ the space of square integrable functions on the domain Ω, and with $H^s(\Omega)$ the standard Sobolev space with norm $\| \cdot \|_s$. Let $H_0^s(\Omega)$ be the space of all functions in $H^s(\Omega)$ that vanish on the boundary of Ω, and with $H^{-s}(\Omega)$ the dual space of $H_0^s(\Omega)$. The trace space for the functions in $H^1(\Omega)$ is denoted by $H^{1/2}(\Gamma)$. The operator $(\cdot, \cdot)$ will denote the $L^2(\Omega(t))$ inner product, and $(\cdot, \cdot)_{\Gamma_s}$ will denote the $L^2(\Gamma_s)$ inner product. We will use the following continuous [11] bilinear and trilinear forms

$$a(\mathbf{u}, \mathbf{v}) = \int_\Omega (\nabla \mathbf{u} + \nabla \mathbf{u}^T) : \nabla \mathbf{v} \, d\mathbf{x} \qquad \forall \mathbf{u}, \mathbf{v} \in \mathbf{H}^1(\Omega) \,, \tag{1}$$

$$b(\mathbf{u}, q) = -\int_\Omega q \nabla \cdot \mathbf{u} \, d\mathbf{x} \qquad \forall q \in L_0^2(\Omega), \forall \mathbf{u} \in \mathbf{H}^1(\Omega) \,, \tag{2}$$

$$c(\mathbf{w}, \mathbf{u}, \mathbf{v}) = \int_\Omega \mathbf{w} \cdot \nabla \mathbf{u} \cdot \mathbf{v} \, d\mathbf{x} \qquad \forall \mathbf{w}, \mathbf{u}, \mathbf{v} \in \mathbf{H}^1(\Omega) \,. \tag{3}$$

The Koiter shell approach relies on the assumptions that the structure displacements are small and normal to the shell surface. The domain of the shell structure is denoted by Γ_s, while the undeformed membrane configuration is indicated with $\Gamma_{s,0}$, the displacement and the external surface forces vectors by $\boldsymbol{\eta}$ and $\mathbf{f_s}$. The weak form of the considered shell equation

results

$$\int_{\Gamma_{s,0}} \rho_s \varepsilon \frac{\partial^2 \boldsymbol{\eta}}{\partial t^2} \cdot \boldsymbol{\psi} \, d\Gamma + \int_{\Gamma_{s,0}} \varepsilon E^{\alpha\beta\lambda\delta} \gamma_{\alpha\beta}(\boldsymbol{\eta}) \gamma_{\lambda\delta}(\boldsymbol{\psi}) \, d\Gamma = \int_{\Gamma_{s,0}} \mathbf{f}_s \cdot \boldsymbol{\psi} \, d\Gamma \,, \tag{4}$$

for appropriate test functions $\boldsymbol{\psi}$ belonging to a functional space to be determined on the basis of the imposed boundary conditions. Furthermore, ρ_s and ε are the density and the thickness of the shell, respectively, and with $E^{\alpha\beta\lambda\delta}$ and $\gamma_{\alpha\beta}$ the elasticity and the change of metric tensor, respectively.

In this work, negligible bend, shear stresses, and linear elastic constitutive law with a homogeneous and isotropic material are considered [3]. Under these hypotheses, the structure model (4) reduces to a simple scalar equation. The dimension of the structure is then reduced by one. So the following simplified model is obtained

$$\rho_s \varepsilon \frac{\partial^2 \eta_n}{\partial t^2} + \beta \eta_n = f_s \qquad \text{on} \quad \Gamma_{s,0} \,,$$
$$\eta_n|_{t=0} = \eta_{n_0} \,, \qquad \left. \frac{\partial \eta_n}{\partial t} \right|_{t=0} = \eta_{n_v} \quad \text{on} \quad \Gamma_{s,0} \,, \tag{5}$$

where η_n represents the displacement normal to the reference solid surface $\Gamma_{s,0}$. The normal displacement field $\boldsymbol{\eta}$ can be written as $\boldsymbol{\eta} = \eta_n \mathbf{n}_0$, where with $\mathbf{n}_0$ we denote the normal unit vector to the reference boundary $\Gamma_{s,0}$.

We consider also prestressed loading along the shell structure

$$\rho_s \varepsilon \frac{\partial^2 \eta_n}{\partial t^2} + \beta^* \eta_n - \nabla \cdot (P \nabla \eta_n) = f_s \quad \text{on} \quad \Gamma_{s,0} \,, \tag{6}$$

where P is the Cauchy stress tensor in the deformed configuration for tangential stresses. The prestressed model (6) must be completed with proper boundary conditions, i.e., $\eta_n|_{\partial\Gamma_{s,0}} = 0$.

The fluid is Newtonian, homogeneous and incompressible, described in ALE form [2, 12] as

$$\rho_f \left. \frac{\partial \mathbf{u}}{\partial t} \right|_{\mathcal{A}} + \rho_f [(\mathbf{u} - \mathbf{w}) \cdot \nabla] \mathbf{u} - \nabla \cdot \boldsymbol{\sigma}^f = \mathbf{0} \quad \text{on} \; \Omega \,,$$
$$\nabla \cdot \mathbf{u} = 0 \qquad\qquad\qquad\qquad \text{on} \; \Omega \,, \tag{7}$$

where ρ_f and $\mathbf{u}$ are the density and the velocity vector of the fluid, and $\boldsymbol{\sigma}^f$ is the Cauchy stress tensor of the fluid written as $\boldsymbol{\sigma}^f = -p\mathbf{I} + \mu(\nabla\mathbf{u} + \nabla\mathbf{u}^T)$, where p and μ are the pressure and the dynamic viscosity of the fluid, respectively. The system of equations (7) is completed with appropriate boundary conditions. The fluid domain is Ω, and $\mathbf{w}$ is the velocity of the points of the fluid domain. On the moving boundaries we have $\mathbf{w}|_{\Gamma_s} = \partial\eta/\partial t$. The velocity $\mathbf{w}$ is extended over the domain by solving the armonic operator $-\Delta\mathbf{w} = 0$ on Ω. Once $\mathbf{w}$ is known, the map which connects each point $\mathbf{x}_0$ of the reference configuration into the deformed configuration $\mathbf{x}_f$ is defined as $\mathbf{x}_f(t) = \mathbf{x}_0 + \int_0^t \mathbf{w} d\tau$.

The structure equations can be reduced to a boundary condition on Γ_s for the fluid problem. Therefore, the two sub-systems (7) and (5) can be coupled by imposing $\boldsymbol{\sigma}^f \cdot \mathbf{n} - f_s \mathbf{n} = 0$ on Γ_s. Let us define the functional space $V^0 = \{\boldsymbol{\phi} \in H^1(\Omega) : \boldsymbol{\phi}|_{\Gamma_D} = \mathbf{0}\}$, where Γ_D is the portion of the boundary where Dirichlet conditions are imposed. In order to satisfy the continuity of the

test functions $\boldsymbol{\phi} \cdot \mathbf{n} = \psi$ over the interface surface Γ_s in the coupled system, a new functional space is introduced as

$$W^0 = \{(\boldsymbol{\phi}, \psi) \in V^0 \times H^1(\Gamma_s) : \ \boldsymbol{\phi} \cdot \mathbf{n} = \psi \text{ over } \Gamma_s\} \ . \tag{8}$$

The optimal control that is introduced in this work is based on the stationary solution of the fluidstructure system. Therefore, in the following, we neglect all the time derivatives. We can write the weak formulation for the coupled system as

$$\begin{aligned}
\rho_f c(\mathbf{u}; \mathbf{u}, \boldsymbol{\phi}) + \mu a(\mathbf{u}, \boldsymbol{\phi}) + b(p, \boldsymbol{\phi}) - (\boldsymbol{\tau}, \boldsymbol{\phi})_{\Gamma \smallsetminus \Gamma_s} + \\
+ (\beta^* J_s \eta_n, \psi)_{\Gamma_s} + (P J_s \nabla \eta_n, \nabla \psi)_{\Gamma_s} = 0 \ , \quad &\forall (\boldsymbol{\phi}, \psi) \in W^0, \\
b(\mathbf{u}, q) = 0 \ , \quad\quad\quad\quad &\forall q \in L^2(\Omega) \ ,
\end{aligned} \tag{9}$$

where $\boldsymbol{\tau} = \boldsymbol{\sigma}^f \cdot \mathbf{n}$, and J_s is defined by the differential transformation $J_s d\Gamma_s = d\Gamma_{s,0}$. A finite element technique is used to obtain the discrete weak formulation of (9). Following [4], we explicitly treat the position of the fluid domain and consider an implicit discretization of the coupling conditions. With this approach, the structural equation can be incorporated into the fluid equations as a Robin boundary condition.

3   Optimal control problem

We now consider the displacement matching optimal control problem. We aim to obtain a given shell deformation, by controlling the fluid velocity on a portion Γ_c of its boundary Γ. Let v_c be the control, such as

$$\mathbf{u} = v_c \mathbf{n}|_{\Gamma_c} \quad \text{on } \Gamma_c \,, \tag{10}$$

thus we assume that the tangential component of the velocity is zero on Γ_c. We introduce the following objective functional

$$\mathcal{J}(\boldsymbol{\eta}, v_c) = \frac{1}{2} \int_{\Gamma_d} |\boldsymbol{\eta} - \boldsymbol{\eta}_d|^2 \, d\Gamma + \frac{\lambda}{2} ||v_c||^2_{H^s(\Gamma_c)} \,, \tag{11}$$

where $\boldsymbol{\eta} = \eta_n \mathbf{n}_0$. The first term expresses the distance in norm between the actual displacement in the normal direction and its desired value $\boldsymbol{\eta}_d$ over the controlled boundary Γ_d, which can either be the whole moving wall or one sub-portion, while the second one has been added to limit the $H^s(\Gamma_c)$-norm of the control, by means of a regularization parameter λ, which weights the importance of the two terms over the cost functional. Choosing a value for it can be challenging: too much regularization leads to smoother but less effective controls, while a lack of regularization may cause numerical issues or non-physical solutions with singularities.

Note that, since $\mathbf{u} \in \mathbf{H}^1(\Omega)$, the natural space where optimal boundary control v_c should be sought is $H^{1/2}(\Gamma_c)$. Usually, the cost term in (11) is modeled as a $H^1(\Gamma_c)$-norm. However, this approach leads to a more restrictive control space than the natural $H^{1/2}(\Gamma_c)$. In this paper, we study and compare the regularization in both spaces, considering $s = 1$ and $s = 1/2$ in (11). Note that $H^1(\Gamma_c)$ is a subspace of $H^{1/2}(\Gamma_c)$.

3.1 Control in $H^1(\Gamma_c)$

If the control belongs to $H^1(\Gamma_c)$, we have that the norm introduced in (11) can be expressed

$$\|v_c\|^2_{H^1(\Gamma_c)} = \|v_c\|^2_{L^2(\Gamma_c)} + |v_c|^2_{H^1(\Gamma_c)},$$

where $|v_c|_{H^1(\Gamma_c)}$ is called seminorm and is given by

$$|v_c|_{H^1(\Gamma_c)} = \Big(\int_{\Gamma_c} |\nabla v_c|^2) d\Gamma \Big)^{1/2}.$$

The functional (11) can be reformulated as

$$\mathcal{J}(\boldsymbol{\eta}, v_c) = \frac{1}{2} \int_{\Gamma_d} |\boldsymbol{\eta} - \boldsymbol{\eta}_d|^2 \, d\Gamma + \frac{\lambda_1}{2} \int_{\Gamma_c} |v_c|^2 d\Gamma + \frac{\lambda_2}{2} \int_{\Gamma_c} |\nabla v_c|^2 d\Gamma, \tag{12}$$

where the regularization parameters λ_1 and λ_2 weights the $L^2(\Gamma_c)$-norm and the $H^1(\Gamma_c)$-seminorm respectively.

We now introduce the following augmented Lagrangian functional $\mathcal{L}$, that is obtained by adding to the objective functional $\mathcal{J}$ the FSI state equations (9) multiplied by the appropriate Lagrangian multipliers, also known as adjoint variables

$$\mathcal{L}(\boldsymbol{\eta}, \mathbf{u}, \mathbf{u}_a, v_c, p_a, \Gamma) = \mathcal{J}(\boldsymbol{\eta}, v_c) + \rho_f c(\mathbf{u}; \mathbf{u}, \mathbf{u}_a) + b(p, \mathbf{u}_a) + b(p_a, \mathbf{u}) + \mu a(\mathbf{u}, \mathbf{u}_a)$$
$$- (\boldsymbol{\tau}, \mathbf{u}_a)_{\Gamma \smallsetminus \Gamma_s} + (\beta^* \boldsymbol{\eta}, \mathbf{u}_a)_{\Gamma_s} + (P\nabla\boldsymbol{\eta}, \nabla\mathbf{u}_a)_{\Gamma_s} + (\mathbf{u} - v_c\mathbf{n}, \mathbf{s}_a)_{\Gamma_c}, \tag{13}$$

where we have used the vector $\boldsymbol{\eta} = \eta_n \mathbf{n}_0$. The stationary points of the Lagrangian functional can be found by setting to zero the Fréchet derivatives taken with respect to all the problem variables. When the derivatives are taken with respect to the adjoint variables the weak form of the state system (9) is recovered as well as the boundary conditions. By taking the derivatives in the direction δp we get

$$\frac{D\mathcal{L}}{Dp}\delta p = b(\delta p, \mathbf{u}_a) - (\delta p \mathbf{n}, \mathbf{u}_a)_{\Gamma \smallsetminus \Gamma_s} = 0 \quad \forall \delta p \in L_0^2(\Omega). \tag{14}$$

From (14), we find that $\nabla \cdot \mathbf{u}_a = 0$ on Ω, and from the surface contributions we recover the boundary conditions $\mathbf{u}_a \cdot \mathbf{n} = 0$ on Γ_D. On Γ_N we have $\delta p = 0$ since we prescribe Neumann boundary conditions with fixed pressure.

For the derivatives in the direction $\delta\boldsymbol{\eta}$, we have

$$\frac{D\mathcal{L}}{D\boldsymbol{\eta}}\delta\boldsymbol{\eta} = (\beta^* \delta\boldsymbol{\eta}, \mathbf{u}_a)_{\Gamma_s} + (P\nabla\delta\boldsymbol{\eta}, \nabla\mathbf{u}_a)_{\Gamma_s} + \int_{\Gamma_d} (\boldsymbol{\eta} - \boldsymbol{\eta}_d) \cdot \delta\boldsymbol{\eta} d\Gamma = 0 \quad \forall \delta\boldsymbol{\eta} \in H^1(\Gamma_s), \tag{15}$$

which gives the boundary conditions on Γ_s for the adjoint velocity. We now collect $\delta\mathbf{u}$ terms and integrate by parts obtaining

$$\frac{D\mathcal{L}}{D\mathbf{u}}\delta\mathbf{u} = \rho_f c(\delta\mathbf{u}; \mathbf{u}, \mathbf{u}_a) + \rho_f c(\mathbf{u}; \delta\mathbf{u}, \mathbf{u}_a) + b(p_a, \delta\mathbf{u}) - \mu(\Delta\mathbf{u}_a, \delta\mathbf{u}) +$$
$$- (\mu\nabla\delta\mathbf{u} \cdot \mathbf{n}, \mathbf{u}_a)_{\Gamma \smallsetminus \Gamma_s} + (\mu\nabla\mathbf{u}_a \cdot \mathbf{n}, \delta\mathbf{u})_{\Gamma} + (\delta\mathbf{u}, \mathbf{s}_a)_{\Gamma_c} = 0, \quad \forall \delta\mathbf{u} \in H^1(\Omega). \tag{16}$$

Then the strong form of the adjoint velocity reads

$$\rho_f(\nabla \mathbf{u})^T \cdot \mathbf{u}_a - \rho_f(\mathbf{u} \cdot \nabla)\mathbf{u}_a + \nabla p_a - \mu \Delta \mathbf{u}_a = 0 \qquad \text{on } \Omega \,, \tag{17}$$

with boundary conditions

$$\mathbf{u}_a = 0 \quad \text{on } \Gamma_D, \qquad (\mu \nabla \mathbf{u}_a \cdot \mathbf{n} + p_a \mathbf{n}) = 0 \quad \text{on } \Gamma_N \cup \Gamma_s \,, \tag{18}$$

and $\mu \nabla \mathbf{u}_a \cdot \mathbf{n} + p_a \mathbf{n} = \mathbf{s}_a$ on Γ_c. Considering the variation δv_c, we have

$$\frac{D\mathcal{L}}{Dv_c}\delta v_c = \lambda_1(v_c, \delta v_c)_{\Gamma_c} + \lambda_2(\nabla v_c, \nabla \delta v_c)_{\Gamma_c} - (\delta v_c \mathbf{n}, \mathbf{s}_a)_{\Gamma_c} = 0 \,, \quad \forall \delta v_c \in H^1(\Gamma_c) \,. \tag{19}$$

Moreover we have to consider the contribution on $\mathcal{L}$ given by the motion of the boundary Γ_s along the direction $\delta \boldsymbol{\eta}$

$$\frac{D\mathcal{L}}{D\Gamma}\delta \boldsymbol{\eta} = \int_{\Gamma_s} \beta^*(\nabla \mathbf{u}_a \cdot \mathbf{n} + \chi \mathbf{u}_a) \cdot \delta \boldsymbol{\eta} \, d\Gamma = 0 \quad \forall \delta \boldsymbol{\eta} \in H^1(\Gamma_s) \,, \tag{20}$$

where χ represents the shell curvature. Under the hypothesis of small deformation we can safely neglect the terms where χ appears. The term with $\mathbf{u}_a$ is defined on the surface Γ_s and a constant extension of this value towards the normal direction to the surface leads to a null normal gradient of this term, so we have that $\frac{D\mathcal{L}}{D\Gamma}\delta \boldsymbol{\eta} = 0$.

3.2 Control in $H^{1/2}(\Gamma_c)$

Before expressing the regularization term by means of the $H^{1/2}(\Gamma_c)$ norm, we first introduce the fractional Sobolev spaces. Given a generic n-dimensional domain $\Omega \subset \mathbb{R}^n$, the fractional Sobolev space $W^{s,p}(\Omega)$ is defined as

$$W^{s,p}(\Omega) = \left\{ u \in L^p(\Omega) : \frac{|u(\mathbf{x}) - u(\mathbf{y})|}{|\mathbf{x} - \mathbf{y}|^{\frac{n}{p}+s}} \in L^p(\Omega \times \Omega) \right\} \,, \tag{21}$$

for any $p \in [1, \infty)$ and with a fractional exponent $s \in (0,1)$. It is an intermediary Banach space between $L^p(\Omega)$ and $W^{1,p}(\Omega)$, endowed with the natural norm

$$\|u\|_{W^{s,p}(\Omega)} = \left(\int_\Omega |u|^p dx + \int_\Omega \int_\Omega \frac{|u(\mathbf{x}) - u(\mathbf{y})|^p}{|\mathbf{x} - \mathbf{y}|^{n+sp}} d\mathbf{x} \, d\mathbf{y} \right)^{\frac{1}{p}} \,, \tag{22}$$

where the term

$$[u]_{W^{s,p}(\Omega)} = \left(\int_\Omega \int_\Omega \frac{|u(\mathbf{x}) - u(\mathbf{y})|^p}{|\mathbf{x} - \mathbf{y}|^{n+sp}} d\mathbf{x} \, d\mathbf{y} \right)^{\frac{1}{p}} \tag{23}$$

is called Gagliardo seminorm. We focus on the case $p = 2$, which is an important case since the fractional Sobolev space $W^{s,2}(\mathbb{R}^n)$ turns out to be the Hilbert space $H^s(\mathbb{R}^n)$ defined as

$$H^s(\mathbb{R}^n) = \left\{ u \in L^2(\mathbb{R}^n) : \frac{|u(\mathbf{x}) - u(\mathbf{y})|}{|\mathbf{x} - \mathbf{y}|^{\frac{n}{2}+s}} \in L^2(\mathbb{R}^n \times \mathbb{R}^n) \right\} \,. \tag{24}$$

We bound this definition on Ω, by saying that $u \in H^s(\Omega)$ if and only if the $\tilde{u} \in H^s(\mathbb{R}^n)$, where the extension function $\tilde{u}$ is defined as [13]

$$\tilde{u}(\mathbf{x}) = \begin{cases} u(\mathbf{x}) & \mathbf{x} \in \Omega, \\ 0 & \mathbf{x} \in \mathbb{R}^n \smallsetminus \Omega. \end{cases} \tag{25}$$

The functional (11) can be expressed as

$$\mathcal{J}(\boldsymbol{\eta}, v_c) = \frac{1}{2}\int_{\Gamma_d} |\boldsymbol{\eta} - \boldsymbol{\eta}_d|^2 \, d\Gamma + \frac{\lambda_1}{2}\int_{\Gamma_c} |v_c|^2 d\Gamma + \frac{\lambda_2}{2}\int_{\mathbb{R}^n}\int_{\mathbb{R}^n} \frac{|v_c(\mathbf{y}) - v_c(\mathbf{x})|^2}{|\mathbf{x} - \mathbf{y}|^{n+1}} dy dx. \tag{26}$$

where the reduction to Γ_c is obtained by imposing

$$v_c = \begin{cases} 0 & \text{on } \mathbb{R}^n \smallsetminus \Gamma_c, \\ v_c & \text{on } \Gamma_c, \end{cases} \tag{27}$$

and n is the dimensionality of Γ_c. Therefore, the derivative of the Lagrangian functional $\mathcal{L}$, obtained by (13) with the objective functional of (26), in the direction δv_c, becomes

$$\frac{D\mathcal{L}}{Dv_c}\delta v_c = \lambda_1(v_c, \delta v_c)_{\Gamma_c} + \lambda_2 \int_{\mathbb{R}^n}\int_{\mathbb{R}^n} \frac{(v_c(\mathbf{y}) - v_c(\mathbf{x}))}{|\mathbf{x} - \mathbf{y}|^{n+1}}(\delta v_c(\mathbf{y}) - \delta v_c(\mathbf{x}))dy dx +$$
$$- (\delta v_c \mathbf{n}, \mathbf{s}_a)_{\Gamma_c} = 0, \quad \forall \delta v_c \in H^{1/2}(\Gamma_c). \tag{28}$$

The integral term over $\mathbb{R}^n$ in (28) is the weak form of the fractional Laplacian of v_c bounded to Γ_c under the hypothesis (27). In this work, the Riesz method is used for the numerical simulations of the fractional Laplacian [14]. Following the approach for the Riesz fractional Laplacian on a bounded domain Γ_c, the term with integrals over $\mathbb{R}^n$ can be split as [15]

$$\int_{\mathbb{R}^n}\int_{\mathbb{R}^n} \frac{(v_c(\mathbf{y}) - v_c(\mathbf{x}))}{|\mathbf{x} - \mathbf{y}|^{n+1}}(\delta v_c(\mathbf{y}) - \delta v_c(\mathbf{x}))dy dy =$$
$$= \int_{\Gamma_c}\int_{\Gamma_c} \frac{(v_c(\mathbf{y}) - v_c(\mathbf{x}))}{|\mathbf{x} - \mathbf{y}|^{n+1}}(\delta v_c(\mathbf{y}) - \delta v_c(\mathbf{x}))dy dx + \tag{29}$$
$$+ 2\int_{\Gamma_c} v_c(\mathbf{x})\delta v_c(\mathbf{x}) \int_{\mathbb{R}^n \smallsetminus \Gamma_c} \frac{1}{|\mathbf{x} - \mathbf{y}|^{n+1}} dy dx.$$

The finite element discretization of (29) is presented in the next section.

4 Numerical results

In this section, we report some numerical results obtained by using the mathematical model shown in the previous sections. Since solving numerically the optimality system in a fully coupled fashion is computationally expensive, we uncouple the state, adjoint, and control equations by using the iterative steepest descent method described in Algorithm 1. The initialization step can be summarized as follows. We first set an initial state $(\mathbf{u}_0, p_0, \eta_0)$ satisfying the state system (9) and compute the initial value of the objective functional $\mathcal{J}_0$ with (12) in the case of $H^1(\Gamma_c)$ control and (26) for the $H^{1/2}(\Gamma_c)$ control. Once the state variables are known, we can solve the

adjoint system (15)-(16) to obtain the adjoint velocity $\mathbf{u}_a$ and the adjoint pressure p_a that are used to compute the value of $\mathbf{s}_a$. Then, the control v_c can be obtained using (19) or (28). A standard line search with backtracking strategy is performed. When the functional decreases under a certain tolerance opt_{tol}, the optimal solution is found and the algorithm stops. We implement the Algorithm 1 in the in-house finite element code FEMuS [16], which works on multiprocessor architectures and uses a multigrid solver with mesh-moving capability.

Algorithm 1 Main sketch of the Steepest Descent algorithm.

---

1. Initialization step.
for $i = 1 \rightarrow i_{max}$ **do**
    2. Solve the system (15)-(16) to obtain the adjoint state $(\mathbf{u}_a, p_a)$
    3. Obtain the control update δv_c^i from (19) or (28) and set $r^i = r^0$
    while $\mathcal{J}^i(v_c^{i-1} + r^i \delta v_c^i, \eta) > \mathcal{J}^{i-1}(v_c^{i-1}, \eta)$ **do**   ▷ *Line search*
        4. r^i update: $r^i = \rho\, r^i$
        5. Solve the state equations (9) with $v_c^i = v_c^{i-1} + r^i \delta v_c^i$
        If $(r^i < toll) \rightarrow$ Line search not successful
        If $\big((\mathcal{J}^i(v_c^i, \eta) - \mathcal{J}^{i-1}(v_c^{i-1}, \eta))/\mathcal{J}^{i-1}(v_c^{i-1}, \eta) < opt_{tol} \rightarrow$ Optimal solution found
    end while
end for

To test the algorithm, we consider a rectangular domain $\Omega = \{(x, y) : x \in [0, 0.1], y \in [0, 0.3]\}$, as shown in Figure 1, and the following boundary conditions. On the boundary $\Gamma_w = \Gamma_D$ we impose no-slip Dirichlet boundary conditions. The velocity control v_c acts on the boundary Γ_c, while on Γ_s we impose the generalized Robin boundary condition to model the structure. On $\Gamma_o = \Gamma_N$ outflow conditions are imposed. We aim to control the displacement of the region $\Gamma_d = \{(x, y) : x = 0.1, y \in [0.08, 0.15]\}$, and we request a fixed desired field $\eta_d = 0.005m$. The fluid has density $\rho^f = 1000\ kg/m^3$ and dynamic viscosity $\mu = 100\ Pa \cdot s$. For the solid, we consider $\beta^* = 60kPa/m$ and thickness $\varepsilon = 0.0075\ m$.

For all the presented simulations, the domain was uniformly divided with a regular rectangular mesh with 10×30 elements. We now introduce the finite element discretization used. Let $X_h^2 \subset H^1(\Omega)$ and $X_h^1 \subset L^2(\Omega)$ be two families of finite-dimensional sub-spaces parameterized by h that tends to zero. To satisfy the BBL inf-sup condition, we consider the velocity $\mathbf{u}_h \in \mathbf{X}_h^2$ and the pressure $p_h \in X_h^1$ and use standard Taylor-Hood elements. We consider a quadratic displacement field $\eta_h \in X_h^2$. The discretization of the adjoint variables follows that of the corresponding state variable.

We describe the finite element approximation of Riesz bounded fractional Laplacian, as presented in [15]. Since the boundary of a two-dimensional case is a one-dimensional domain, the mixed integral for the Riesz assembly can be reduced to

$$
\begin{aligned}
2\int_{\Gamma_c} v_c(x)\delta v_c(x) \int_{\mathbb{R}\setminus\Gamma_c} \frac{1}{(x-y)^2}dy\,dx &= \\
= 2\int_{\Gamma_c} v_c(x)\delta v_c(x)\Big(\int_{-\infty}^{e_1} \frac{1}{(x-y)^2}dy + \int_{e_2}^{\infty} \frac{1}{(x-y)^2}dy\Big)dx &= \\
= 2\int_{\Gamma_c} v_c(x)\delta v_c(x)\Big(\frac{1}{x-e_2} - \frac{1}{x-e_1}\Big)dx\,,
\end{aligned}
\tag{30}
$$

where e_1 and e_2 are the extremes of the Γ_c. The first double integral in (29) is discretized as

$$
\int_{\Gamma_c} \int_{\Gamma_c} \frac{v_c(y) - v_c(x)}{(x-y)^2} \big(\delta v_c(y) - \delta v_c(x)\big) \, dy dx \simeq
$$
$$
\simeq \sum_{el_x=1}^{N_{el}} \sum_{x_g=0}^{n_g(el_x)} J_{x_g} w_{x_g} \left(\sum_{el_y=1}^{N_{el}} \sum_{y_g=0}^{n_g(el_y)} J_{y_g} w_{y_g} \frac{v_{c,h}(y_g) - v_{c,h}(x_g)}{(x_g - y_g)^2} \big(\delta v_c(y_g) - \delta v_c(x_g)\big) \right),
$$

(31)

and (30) is discretized as

$$
2 \int_{\Gamma_c} v_c(x) \delta v_c(x) \Big(\frac{1}{x-e_2} - \frac{1}{x-e_1} \Big) dx \simeq
$$
$$
\simeq \sum_{el_x=1}^{N_{el}} \sum_{x_g=0}^{n_g(el_x)} 2 J_{x_g} w_{x_g} v_{c,h}(x_g) \delta v_{c,h}(x_g) \Big(\frac{1}{x_g - e_2} - \frac{1}{x_g - e_1} \Big),
$$

(32)

where all the loops are developed on the boundary elements.

Since the Riesz approach is nonlocal, the numerical system to be solved is characterized by a dense matrix. The resolution of a dense matrix is numerically expensive, so the resolution of these operators over complex domains might be unfeasible. In our case, the computation is limited to the boundary element of Γ_c. For this purpose, we used the PETSc libraries, that support the resolution of numerical systems characterized by dense matrices.
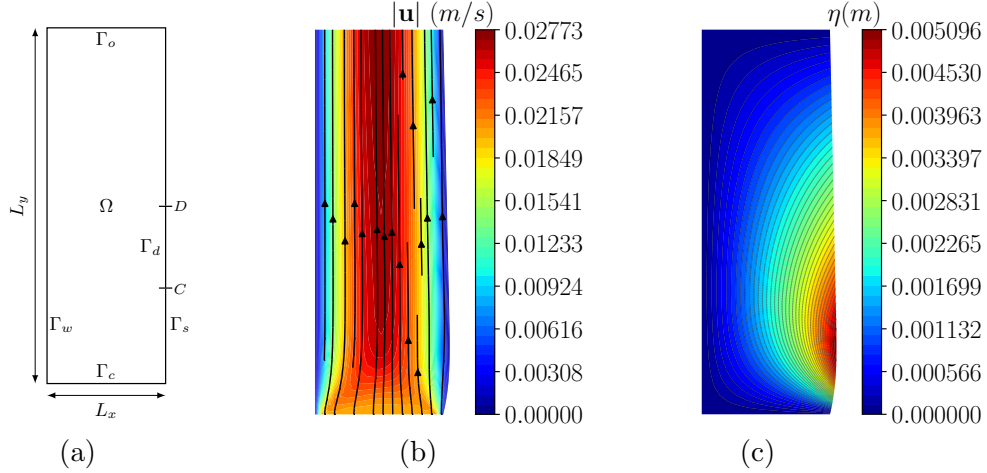

Figure 1: Geometry used for the numerical test (a). Contours and streamlines of the velocity field (b) and contours of the displacement (c) for the reference case.

The objective of our problem is to control the normal displacement on the surface Γ_d of the membrane by acting on the fluid through the normal fluid velocity v_c on the boundary Γ_c. We consider two different cases: the velocity v_c belonging to the space $H^1(\Gamma_c)$ and to the natural space $H^{1/2}(\Gamma_c)$. Several tests have been performed by considering $\lambda_1 = 10^{-9}$ and various values for λ_2. In Table 1 we report the functional values and the number of iterations done by the

Table 1: Objective functional values, number of algorithm iterations obtained with different λ_1 values, for $\lambda_2 = 10^{-9}$, $v_c \in H^1(\Gamma_c)$ and $v_c \in H^{1/2}(\Gamma_c)$.
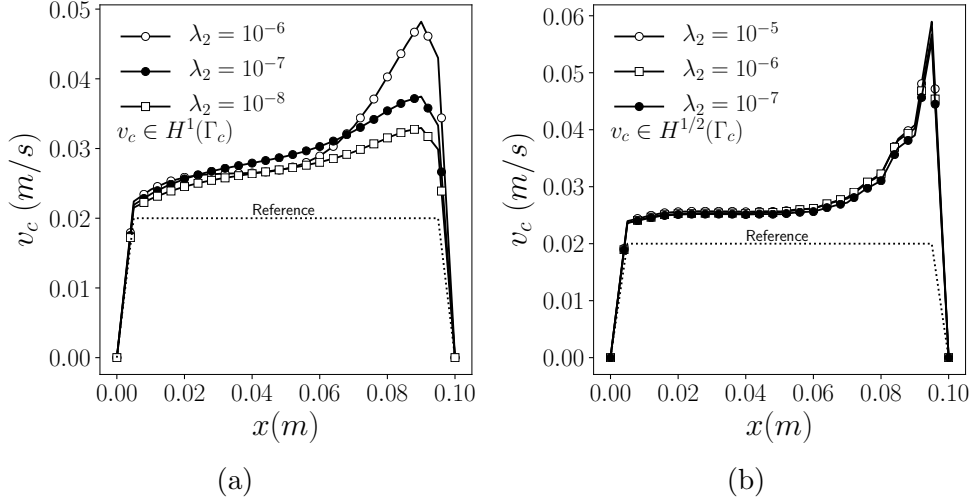
	$v_c \in H^1(\Gamma_c)$		$v_c \in H^{1/2}(\Gamma_c)$	
λ_2	$\mathcal{J}(\eta, v_c)$	Iterations	$\mathcal{J}(\eta, v_c)$	Iterations
Reference	$1.3718 \cdot 10^{-9}$	-	$1.3718 \cdot 10^{-9}$	-
10^{-6}	$4.91889 \cdot 10^{-10}$	2	$3.16288 \cdot 10^{-10}$	3
10^{-7}	$3.05569 \cdot 10^{-10}$	5	$2.69857 \cdot 10^{-10}$	2
10^{-8}	$2.05425 \cdot 10^{-10}$	18	$1.11873 \cdot 10^{-9}$	18

(a)   (b)
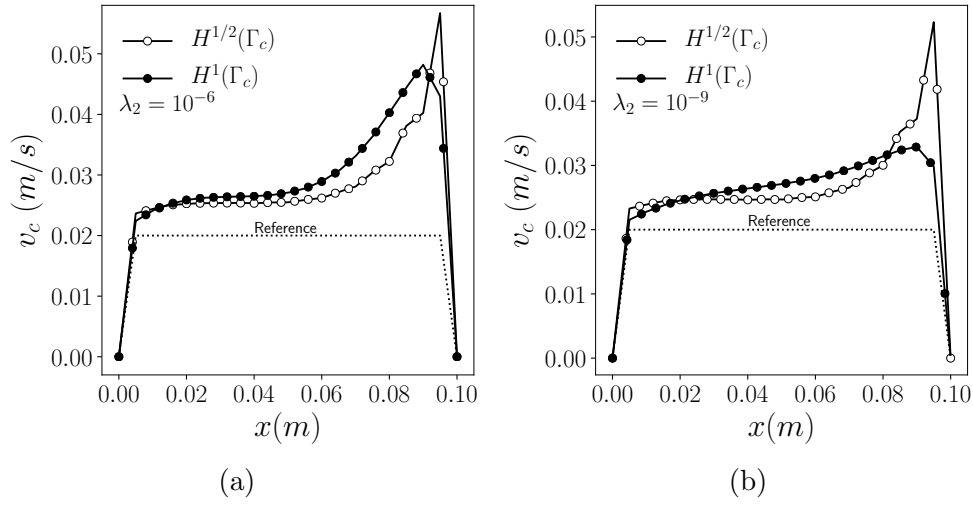
Figure 2: Comparison of the velocity v_c profile along the controlled boundary Γ_c for $H^1(\Gamma_c)$ and $H^1(\Gamma_c)$. Optimal solution for $\lambda_2 = 10^{-6}$ (a) and $\lambda_2 = 10^{-9}$ (b).

algorithm to obtain the optimal solutions as a function of the regularization parameter λ_2 for both regularizations.

By reducing the control regularization, we notice that the optimal solutions tend to the desired one after a larger number of iterations. The velocity v_c over the controlled boundary Γ_c is shown in Figure 2 and 3 for $\lambda_2 = 10^{-6}$ and $\lambda_2 = 10^{-9}$ and both regularization. The distance from the objective decreases as the value of λ_2 decreases, consistently with the expectations. Moreover, the results obtained with the fractional regularization show a slightly lower distance from the objective in comparison with the $H^1(\Gamma_c)$ regularization, as expected from the theoretical results: in fact, the $H^1(\Gamma_c)$ regularization imposes the solution in a more restrictive function space than the natural one.

Figure 3: Comparison of the velocity v_c profile along the controlled boundary Γ_c for $\lambda_2 = 10^{-7}, 10^{-8}, 10^{-9}$ with $v_c \in H^1(\Gamma_c)$ (a) and $\lambda_2 = 10^{-5}, 10^{-6}, 10^{-7}$ with $v_c \in H^{1/2}(\Gamma_c)$.

5   Conclusions

In this work, we presented and compared two different regularization methods for the treatment of Dirichlet boundary optimal control problems for a steady multiscale fluid-structure interaction system. The optimization problem aims to achieve the desired deformation of the membrane modeled through the Koiter shell model, by acting on the velocity field on a portion of the boundary. We have obtained the optimality system, and the optimal control problem has been solved by using the Lagrange multiplier method and the gradient of functional has been determined by solving the adjoint problem. We first implemented a standard H^1-norm for the regularization of the velocity. However, this approach leads to solutions in a more restrictive control space than the natural one. The second formulation we proposed limits the $H^{1/2}$-norm of the control parameter, then the control parameter is sought in its natural space. This approach requires the numerical approximation of the fractional Laplacian operator, which we performed by directly applying the Riesz method. We performed numerical simulations on a finite element framework, considering both regularization approaches and studying the influence of the regularization coefficients. All the performed simulations show a decrease in the distance from the objective, thus effectively controlling the displacement field through the inlet velocity. In addition, the fractional approach shows a smaller distance from the objective in comparison with the H^1 regularization, as theoretically expected.

REFERENCES

[1] S. Turek and J. Hron, "Proposal for numerical benchmarking of fluid-structure interaction between an elastic object and laminar incompressible flow," *Lecture notes in computational science and engineering*, vol. 53, p. 371, 2006.

[2] L. Formaggia, A. Quarteroni, and A. Veneziani, *Cardiovascular Mathematics: Modeling and simulation of the circulatory system*, vol. 1. Springer Science & Business Media, 2010.

[3] W. Koiter, "On the mathematical foundation of shell theory," in *Proc. Int. Congr. of Mathematics, Nice*, vol. 3, pp. 123–130, 1970.

[4] F. Nobile and C. Vergara, "An effective fluid-structure interaction formulation for vascular dynamics by generalized robin conditions," *SIAM Journal on Scientific Computing*, vol. 30, no. 2, pp. 731–763, 2008.

[5] M. D. Gunzburger, *Perspectives in flow control and optimization*, vol. 5. Siam, 2003.

[6] M. D. Gunzburger and S. Manservisi, "Analysis and approximation of the velocity tracking problem for navier–stokes flows with distributed control," *SIAM Journal on Numerical Analysis*, vol. 37, no. 5, pp. 1481–1512, 2000.

[7] L. Chirco and S. Manservisi, "An adjoint based pressure boundary optimal control approach for fluid-structure interaction problems," *Computers & Fluids*, vol. 182, pp. 118–127, 2019.

[8] T. Richter and T. Wick, "Optimal control and parameter estimation for stationary fluid-structure interaction problems," *SIAM Journal on Scientific Computing*, vol. 35, no. 5, pp. B1085–B1104, 2013.

[9] A. Chierici, L. Chirco, and S. Manservisi, "Optimal pressure boundary control of steady multiscale fluid-structure interaction shell model derived from koiter equations," *Fluids*, vol. 6, no. 4, p. 149, 2021.

[10] G. Bornia, A. Chierici, and S. Ratnavale, "A comparison of regularization methods for boundary optimal control problems," *International Journal of Numerical Analysis and Modeling*, vol. 19, no. 2-3, pp. 329–346, 2022.

[11] P. G. Ciarlet, *The finite element method for elliptic problems*. SIAM, 2002.

[12] T. J. Hughes, W. K. Liu, and T. K. Zimmermann, "Lagrangian-eulerian finite element formulation for incompressible viscous flows," *Computer methods in applied mechanics and engineering*, vol. 29, no. 3, pp. 329–349, 1981.

[13] M. DElia, Q. Du, C. Glusa, M. Gunzburger, X. Tian, and Z. Zhou, "Numerical methods for nonlocal and fractional models," *Acta Numerica*, vol. 29, pp. 1–124, 2020.

[14] A. Lischke, G. Pang, M. Gulian, F. Song, C. Glusa, X. Zheng, Z. Mao, W. Cai, M. M. Meerschaert, M. Ainsworth, *et al.*, "What is the fractional laplacian? a comparative review with new results," *Journal of Computational Physics*, vol. 404, p. 109009, 2020.

[15] G. Barbi, D. Capacci, A. Chierici, L. Chirco, V. Giovacchini, and S. Manservisi, "A numerical approach to the fractional laplacian operator with applications to quasi-geostrophic flows," in *Journal of Physics: Conference Series*, vol. 2177, p. 012013, 2022.

[16] A. Chierici, G. Barbi, G. Bornia, D. Cerroni, L. Chirco, R. Da Vià, V. Giovacchini, S. Manservisi, R. Scardovelli, and A. Cervone, "Femus-platform: a numerical platform for multiscale and multiphysics code coupling," in *9th edition of the International Conference on Computational Methods for Coupled Problems in Science and Engineering*, 2021.